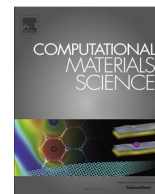




Contents lists available at ScienceDirect

## Computational Materials Science

journal homepage: [www.elsevier.com/locate/commatsci](http://www.elsevier.com/locate/commatsci)

# Simulation of the fracture behavior of Al6061 laser welded joints with the Rousselier model

H.Y. Tu\*, S. Schmauder, U. Weber

*Institute for Materials Testing, Materials Science and Strength of Materials (IMWF), University of Stuttgart, Pfaffenwaldring 32, D-70569 Stuttgart, Germany*

## ARTICLE INFO

### Article history:

Received 11 June 2015

Received in revised form 23 October 2015

Accepted 24 October 2015

Available online xxxx

### Keywords:

Aluminum laser welded joints

Rousselier model

Crack propagation

FE simulation

## ABSTRACT

Ductile fracture behavior of an aluminum laser beam welded joint is investigated experimentally and numerically. Based on the hardness test across the welded joints, the dimensions of different weld regions are fixed. Tensile tests of flat specimens extracted from the base material, from the fusion zone and from the heat affected zone are made. The mechanical properties of the different weld regions are used as finite element model input in the simulation work. Fracture toughness tests are performed on compact tension specimens with the initial crack located in the base material, and in the center of the fusion zone, respectively. The tensile test results of compact tension specimens are shown in the form of force vs. crack opening displacement and fracture resistance curves. Based on the numerical calibration of the Rousselier parameters on notched round specimens, the Rousselier model is used to investigate the crack propagation of the compact tension specimen. Good agreement between the numerical and experimental results is obtained from compact tension specimens with the initial crack located at different positions of the weld region.

© 2015 Elsevier B.V. All rights reserved.

## 1. Introduction

Aluminum alloys (around 1/3 density of steel) are used widely in automotive and aircraft industries due to their excellent mechanical and high strength to weight ratio in order to save structural material and fuel. In aerospace industries, 6xxx aluminum alloys considered as potential replacement alloys for Al2024 have wide application in the fuselage [1]. In comparison to Al2024, 6xxx aluminum alloys (e.g., Al6061 alloy) has its advantages, e.g., higher strength and better weldability. Due to the requirement of lighter structures in aerospace industry, aluminum weldments are used widely instead of the riveting in airplane production. Accompanying the application of Al6061 welded joints in aircraft industry, many numerical and experimental studies have been performed to focus on the mechanics of Al6061 welded joints [2–4].

Advanced welding techniques, such as friction stir welding and laser beam welding have found many applications in aluminum alloys [5–9]. As the application of the welded joints, the fracture behavior of the welded joints is investigated experimentally and numerically as the fracture behavior of the welded joints influence the serving life of the component. Some damage models, e.g., the

Gurson–Tvergaard–Needleman (GTN) model [10–12] and the Rousselier model [13,14] were used to study the ductile fracture behavior of a laser welded joint [15–18], a friction stir welded aluminum joint [19–20] and an electron beam welded steel joint [21]. In comparison to the GTN model, the Rousselier model is easier to use as it possesses less model parameters and can predict similar simulation results [21,22]. Since the Rousselier model has successfully been used to predict the ductile fracture of the AA2050 aluminum alloy [23], Al5052 [24] and the ductile fracture of an electron beam welded steel joint [21], it is interesting to apply the Rousselier model to study the fracture behavior of aluminum laser beam welded joints.

## 2. Experimental investigations

In this paper, 8 mm thick Al6061-T651 (T651 temper: Solution-heat-treated, water-quenched and aged and stress-relieved by stretching) plates were laser welded with a 6 kW CO<sub>2</sub> laser beam and butt welded joints are obtained. The chemical components of Al6061-T651 obtained by spectrometric analysis at five random measurement points are shown in Table 1 [4].

In order to identify different weld regions, especially the fusion zone (FZ) and the heat affected zone (HAZ), microhardness (HV0.2) was measured across the welded joint. The hardness measurements were performed across the weld regions at four test

\* Corresponding author.

E-mail address: [haoyun.tu@imwf.uni-stuttgart.de](mailto:haoyun.tu@imwf.uni-stuttgart.de) (H.Y. Tu).

**Table 1**  
Chemical composition of the Al6061-T651, mass contents in % [4].

Element	Si	Fe	Cu	Mn	Mg	Cr	Zn	Ti	B	Zr	Al
(wt%)	0.698	0.437	0.269	0.117	0.878	0.120	0.143	0.037	<0.005	<0.005	Balance

locations in order to avoid the initial defects in the fusion zone, as shown in Fig. 1. Every 0.2 mm a measurement was performed in order to define the Vickers hardness values of different weld regions. The hardness profile across the welded joint is shown in Fig. 1. The fusion zone possesses the lowest hardness value (59–75 HV0.2), whereas the base material (BM) attains the highest hardness value around 108 HV0.2 (104–113). From the hardness test profile cross the welded joint, the average dimensions of the FZ and the HAZ are found to be 3.6 mm and 6 mm, respectively.

As the dimensions of the FZ and the HAZ are small, it is not possible to extract round specimens from these narrow regions. Flat specimens were manufactured from each weld region and tensile tested in order to get mechanical properties of different weld areas. These flat specimens have a thickness of 1 mm, a width of 5 mm and a gauge length of 25 mm. After the tensile process, engineering stress–strain curves of different weld regions of Al6061 laser welded joints are shown in Fig. 2. The yield stress of the FZ is around 50% lower than that of the BM and the tensile strength  $\sigma_m$  for FZ is lowest in the three regions. The base material possesses the highest yield stress and the flat specimen obtained from the BM ruptures at low ductility (around 12% deformation). The HAZ is a transitional area where the mechanical property is between that of the BM and the FZ. Table 2 shows the mechanical properties of the welded joints containing yield stress  $\sigma_0$ , tensile strength  $\sigma_m$ , uniform strain  $A_g$  and strain at rupture  $A$ , both for Al6061 base material and fusion zone. Notched round specimens with 2 mm notch radius (named: 2NB1-3) and 4 mm notch radius (named: 4NB1-3) were produced from the BM, the dimensions of which are shown in Fig. 3. Tensile tests were performed at room temperature, in which the gauge length is 20 mm. During the tensile test process, force vs. cross section reduction curves were recorded. The experimental force vs. diameter reduction curves will be used for the calibration of the Rousselier parameters later.

In order to define the volume fraction of inclusions, optical microscope investigations on the polished surfaces of the specimens were performed, both for the BM and the FZ. Typical microscopy pictures of different weld regions are shown in Fig. 4 (a) and (b). As mentioned in the previous work [4], for the BM, both the Al–Mn–Si phase and iron-rich particle play the role of

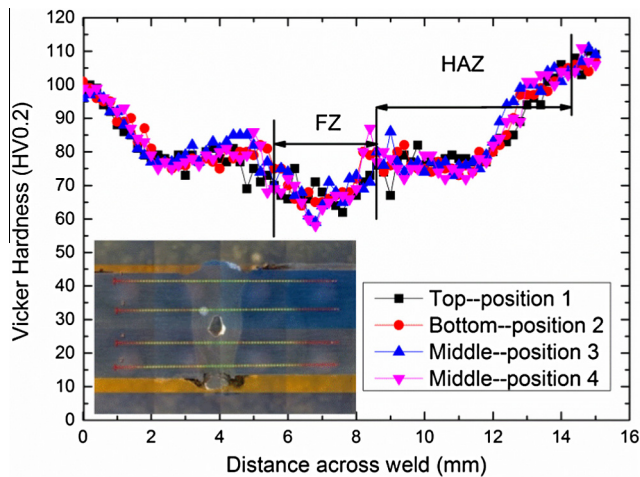


Fig. 1. Vicker hardness profile of the laser beam welded joint.

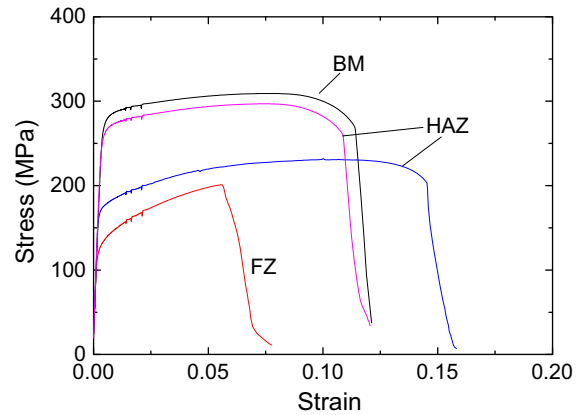


Fig. 2. Engineering stress–strain curves obtained from tensile test results of flat specimens extracted from different weld regions of Al6061 laser beam welded joints.

**Table 2**  
Mechanical properties of different weld regions of Al6061 laser beam welded joint.

$\sigma_0^{BM}$ (MPa)	$\sigma_0^{FZ}$ (MPa)	$\sigma_m^{BM}$ (MPa)	$\sigma_m^{FZ}$ (MPa)	$A_g^{BM}$	$A_g^{FZ}$	$A^{BM}$	$A^{FZ}$
290.6	131.1	316.8	201.0	0.071	0.056	0.126	0.077

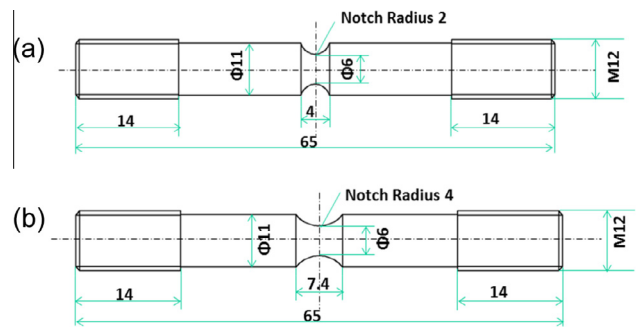


Fig. 3. Sketches of notched round specimens with (a) 2 mm notch radius and (b) 4 mm notch radius.

inclusions which nucleate voids under external tensile loading conditions. The volume fraction of inclusions ( $f_0$ ) for the BM is found as 0.0134 and the average distance between the neighboring inclusions  $l_c$  which derived from experiments is 0.07 mm, the value of  $f_0$  for the FZ is 0.02 and  $l_c$  = 0.01 mm.

Fracture toughness tests of Al6061 laser beam welded joints were performed with compact tension (C(T)) specimens with width  $W$  = 50 mm and the thickness  $B$  = 6 mm. A notch was machined by the Electron Discharge Machining up to a length of  $0.44W$  ( $a/W$  = 0.44), then the specimen was fatigue loaded up to the initial crack length ( $a_0/W$  = 0.52). In order to investigate crack propagation at different weld regions, C(T)-specimens were manufactured with different configurations, i.e., the initial crack was located in the BM (C(T)-BM) and in the middle of the FZ (C(T)-FZ). After the C(T) test, the experimental results are shown in terms of force vs. Crack Opening Displacement (COD) as well as fracture resistance  $J_R$ -curves, as shown in Fig. 5. The crack

Download English Version:

<https://daneshyari.com/en/article/1559992>

Download Persian Version:

<https://daneshyari.com/article/1559992>

[Daneshyari.com](https://daneshyari.com)